ELSEVIER

Ecological Modelling 139 (2001) 1–15

ECOLOGICAL MODELLING

www.elsevier.com/locate/ecolmodel

# Effects of global climate change on coastal salt marshes

T. Simas, J.P. Nunes, J.G. Ferreira *

*IMAR — Center for Ecological Modelling, Departmento de Ciências e Engenharia do Ambiente, Faculdade de Ciências e Tecnologia, Universidade Nova de Lisboa-Qta. da Torre, 2825 Monte de Caparica, Portugal*

Received 10 February 2000; received in revised form 24 October 2000; accepted 14 November 2000

**Abstract**

A methodology combining ecological modelling with geographical information analysis and remote sensing was employed to determine the effects of sea-level rise in estuarine salt marshes, using the Tagus estuary (Portugal) as a case study. The development of salt marsh vegetation was simulated separately for C3 and C4 plants, using a combined biogeochemical and demographic model. This simulation, which provided small-scale ($m^2$) results of annual above-ground primary production, was upscaled to the whole salt marsh area, using bathymetry data, remote sensing and Geographic Information System (GIS) for assessing vegetation cover and determining areal distribution of C3 and C4 vegetation. Based on IPCC data, several sea-level rise scenarios were considered, and the coupled ecological model-GIS were applied to these in order to determine changes in global salt marsh productivity. The results indicate that the salt marshes of the mesotidal estuaries such as the Tagus are susceptible to sea-level rise only in a worst case scenario, which is more likely to occur if the terms set out by the Kyoto protocol are not met by several industrialised nations. The low vulnerability of salt marshes supports the suggestion that areas with high tidal ranges are less vulnerable to sea level change, due to greater sediment transport and accretion. Nevertheless, the precautionary principle should always be applied by coastal planners, due to the great uncertainty surrounding forecasts of sea-level rise. 

*Keywords:* Global warming; Salt marsh; Benthic primary production; Sea-level rise; Remote sensing; GIS; Ecological modelling; Tagus estuary

## 1. Introduction

The enhanced greenhouse effect is well documented (e.g. IPCC, 1990; Titus and Narayanan, 1995). It is the result of a recent increase in the atmospheric concentration of the main greenhouse gases, carbon dioxide; methane and nitrous oxide. This change has a Human origin — during the last 250 years, industrial activity has been increasing and with it the combustion of fossil fuels (such as coal, oil, and gas), which produce these gases (Houghton, 1999). This problem was first posed in the mid 1960s, when it was demonstrated that greenhouse gases were accumulating in the atmosphere (Titus et al., 1991).

* Corresponding author. Tel.: +351-21-2948300 ext. 10117; fax: +351-21-2948554.

*E-mail address:* jgferreira@compuserve.com (J.G. Ferreira).

0304-3800/01/$ - see front matter 
PII: S0304-3800(01)00226-5

The climatic response to the enhanced greenhouse effect is calculated by means of highly complex General Circulation Models (GCMs), assuming the doubling of the pre-industrial atmospheric $CO_2$ concentration (the main greenhouse gas). According to the reports of the Intergovernmental Panel on Climate Change (IPCC) in 1990, confirmed in 1995, the global average temperature will rise by about 2.5°C, with a range of 1.5–4.5°C, depending on the model used (Berner and Berner, 1996; Houghton, 1999; IPCC, 1999). These results are still uncertain, however, due to the natural temperature variability from place-to-place, day-to-day, and season-to-season, as well as to uncertainties with modelling (Gates, 1993; Houghton, 1999).

A rise in average sea-level is another expected consequence of the enhanced greenhouse effect, both because of oceanic thermal expansion, and the melting of Arctic and Antarctic glaciers (Titus et al., 1991). The uncertainties in estimates about future global sea-level rise are substantial. The estimates for sea-level rise by 2100, made since 1983 by several authors, range from 0 to 350 cm (Titus and Narayanan, 1995). This could be due to the uncertain amount of temperature rise, as well as due to the different model estimates given for the amount of sea level rise due to the melting of glaciers and small ice caps. However, according to the estimates of IPCC the total average sea-level rise is predicted to be about 12 cm by 2030 and about 50 cm by the year 2100 (Houghton, 1999; IPCC, 1999).

Temperature increase and sea-level rise will have important impacts on aquatic ecosystems. In Regions of Restricted Exchange (RREs), such as estuaries, barrier islands and lagoons, benthic systems are especially affected by sea-level rise through inundation, while pelagic production is mainly affected by temperature change, which could lead to a net photosynthesis increase (Gates, 1993), as well as a rise in respiration rates. Since respiration releases $CO_2$ to the atmosphere, the increase of respiration rate with temperature could represent a positive feedback on global warming (Gates, 1993).

Salt marshes are coastal ecosystems developed in temperate zones, mainly occupied by halophytic vegetation and exposed to low hydrodynamic conditions and tidal flooding. Ecologically, salt marshes are characterised by their high primary productivity and species diversity, representing habitat for migratory waterfowl, transient fish species and indigenous flora and fauna. Commercially, these ecosystems provide important resources as nursery grounds for several fish and crustacean fisheries (Reed, 1990; Van Dijkeman et al., 1990). Tidal amplitude, in relation to slope and elevation of the shore, is a determining factor for the location of salt marshes. Salt marsh vegetation is located in areas receiving both inundation by sea water and exposure to air, as well as having an adequate soil salinity and chemistry (Eleuterius and Eleuterius, 1979).

Since salt marshes are described as transition zones between land and sea, they are also particularly vulnerable to sea-level rise — as the sea rises, the outer salt marsh boundary will erode and new salt marsh will form inland. According to Reed (1990), the response of coastal marshes to relative sea-level rise depends upon their ability to maintain their relative elevation through sedimentation, areas where the sedimentation rate is in excess of sea-level rise are considered areas of positive balance. These areas are frequently associated with estuarine marshes of rivers with high sediment discharge. Conversely, where relative sea-level rise exceeds coastal marsh sedimentation, erosion processes take place and flooding is inevitable; an 'elevation deficit' occurs (Hackney and Cleary, 1987; Boumans and Day, 1993; Reed and Foote, 1997). Examples of these systems are related to dammed rivers like the Mississippi and the Nile. Finally, tidal range is considered by Stevenson et al. (1986) to be an important indicator of potential sediment transport, suggesting that areas with high tidal ranges are less vulnerable to sea-level change.

Salt-marshes are able to react to sea-level rise by a negative feedback mechanism — a small increase in sea level leads to greater mineral deposition due to extended submersion time, and to reduced soil compaction due to reduced decomposition of organic matter in the soil (Nyman et al., 1993; Allen, 1994). However, rapid sea-level rise can counteract this negative feedback with a posi-

tive one that actually increases salt-marsh loss, increased submersion times reduce salt marsh production and, therefore, organogenic sedimentation (Nyman et al., 1993; Nyman et al. 1994). In fact, there are signs that organogenic sedimentation should be greater than sea-level rise, in order to assure the continued existence of the salt marsh (Allen, 1990a,b); mineralogic sedimentation is dependent, not only on greater submersion periods, but also on available sediment in the system, which might not be sufficient to keep pace with sea-level rise (Cahoon et al., 1995). Although these two feedback processes are understood, their modelling is still qualitative and exploratory, with little quantitative reliability (Nyman et al., 1994; Allen, 1997). Sedimentation of organic matter is considered constant (Allen, 1990b, 1994, 1995), correlated with mineralogic deposition (Woolnough et al., 1995), or correlated with primary production, a process that requires extensive calibration with field data (Day et al., 1999).

The objective of this work is to examine the consequences of sea-level rise in salt marsh areas, using an approach combining ecological modelling, remote sensing, and geographical information analysis. The methodology developed in this paper allows the representation of vegetation growth and population dynamics at a small-scale ($m^2$), and an accurate upscaling to entire salt marsh areas by analysing vegetation cover and bathymetry.

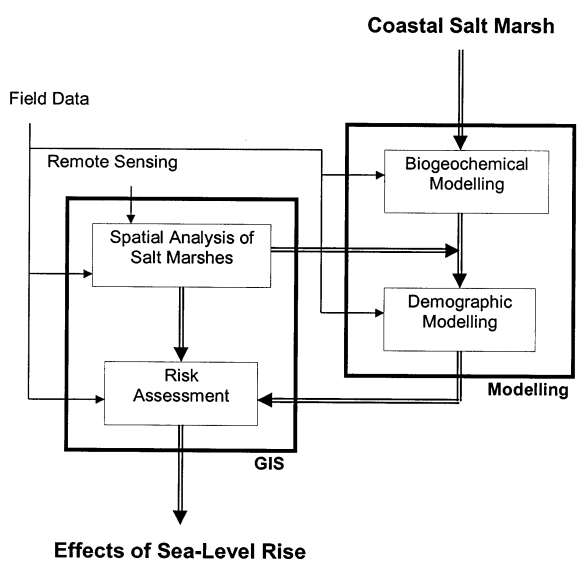


Fig. 1. Methodology used for the integration of modelling and GIS approaches.

## 2. Methodology

The relationship between the different components of this work is shown in Fig. 1.

Data gathering was made by analysing the field data described in the literature, and by remote sensing of the study area. Firstly, a coupled biogeochemical and population-dynamics model was built describing the main ecological processes of salt marsh vegetation per unit of area. In parallel, an initial spatial analysis of the salt marsh area was conducted using Geographic Information System (GIS) tools on geographical data (both satellite imagery and field data). This information also allowed the development of sea-level rise scenarios. The model was then upscaled using the spatial analysis data, in order to give results for the full salt marsh area. Finally, the model results were further analysed with GIS, giving them a spatial dimension.

### 2.1. Study area

The Tagus estuary is one of the largest in Europe, covering an area of about 320 $km^2$ (Fig. 2). Forty percent of this value corresponds to intertidal zones, where about 20 $km^2$ are occupied by salt marsh vegetation (Crespo, 1993; Caçador, 1994). This ecosystem forms the major part of the Tagus Estuary Natural Reserve; only the salt marshes belonging to the Reserve were object of this study. Table 1 compares the study area with other estuarine salt marshes.

This area was chosen because it can represent a wide range of different estuarine salt marshes. An average-sized salt marsh area thrives under mesotidal conditions (tidal range of 1–4 m). Halophytic succession is similar to other salt marshes — lower areas are dominated by *Spartina* species while the upper areas are dominated by other species more resistant to saline conditions, *Halimione portulacoides* and *Arthroc-*

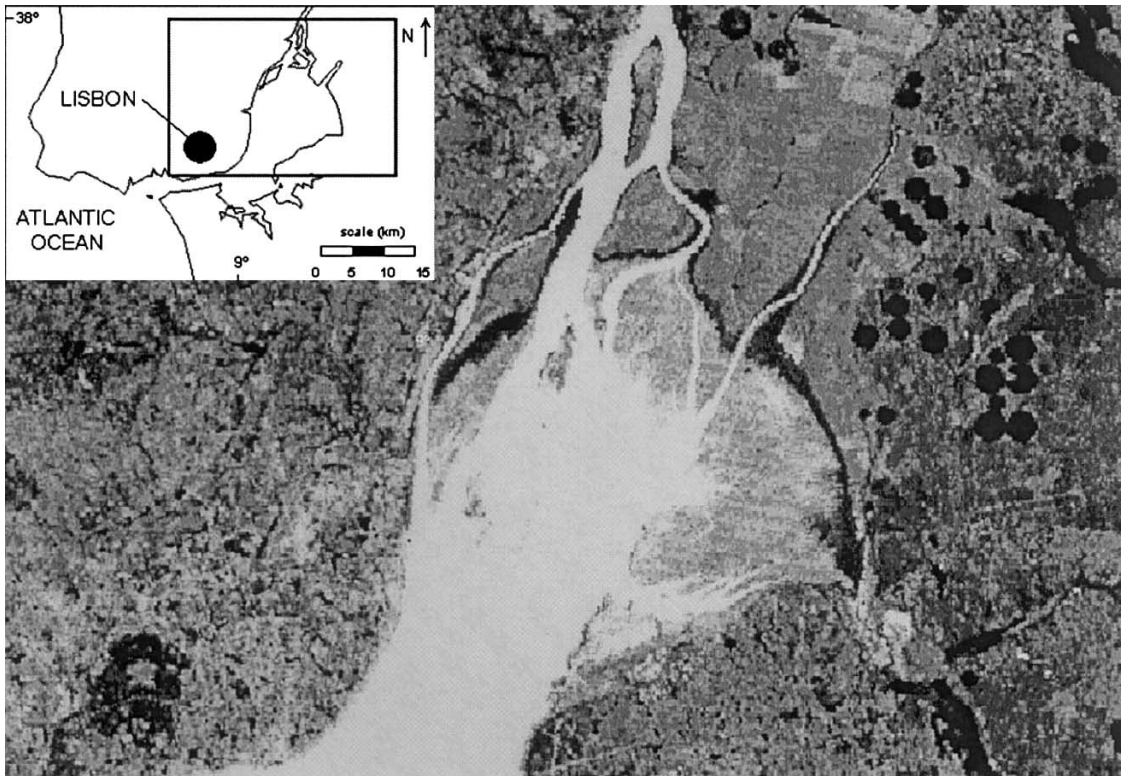


Fig. 2. Correlation between observed (Catarino and Caçador, 1981) and simulated biomass per unit area (g dw $m^{-2}$). Mean standard deviation of observed values (not shown) was estimated at about 640 g $m^{-2}$ for the lower marsh and about 1000 g $m^{-2}$ for the upper marsh.

*nemum fruticosum*. Soil composition in the salt marsh areas is mainly of mineral nature with a fine fraction of 40–60% while organic matter levels correspond to about 10–20%.

### 2.2. Model development

Salt marsh vegetation processes were simulated by combining a biogeochemical model and a demographic model. The former addresses the physiological processes at the individual level, and the latter the population dynamics of salt marsh plants. The two models were developed for the aboveground vegetation part and are described below.

#### 2.2.1. Biogeochemical model

In this model, biomass variation can be simulated for two pathways of carbon assimilation, $C_3$ and $C_4$ (Eq. (1)).

$$\frac{\partial B}{\partial t} = P_g - R - L_m - E \quad (1)$$

where $P_g$, gross production; $R$, respiration; $L_m$, leaf mortality; $E$, exudation. Gross production is represented by Eq. (2).

$$P_g = P_{max\ wt} \cdot f(I) \cdot f(T) \cdot f(N) \quad (2)$$

where $P_{max\ wt}$, maximum allometric production of $C_3$ or $C_4$ species; $f(I)$, light intensity function; $f(T)$, air-temperature function; $f(N)$, nutrient function.

$P_{max\ wt}$ is the maximum production rate of $C_3$ and $C_4$ species at light saturation (Table 2), implemented as an allometric function. Available light energy is modelled according to Brock (1981), and

for each plant biomass class, the potential production is calculated using Eq. (3) based on the half-saturation light intensity for $C_3$ and $C_4$ species and on hourly photosynthetically active radiation on the leaf surface

$$f(I) = \frac{I}{(I_k + I)} \quad (3)$$

where $I$, light intensity; $I_k$, half-saturation constant for solar radiation.

The air-temperature function is described by a temperature coefficient for growth (Bach, 1993) dependent on temperature optimum for $C_3$ and $C_4$ salt marsh species and hourly air-temperature variation

$$f(T) = \theta_1^{(T - T_{opt})} \quad (4)$$

where $\theta_1$, temperature coefficient for growth; $T$, air-temperature; $T_{opt}$, temperature optimum for growth.

The nutrient limitation function is based on a cell-quota model that calculates the intracellular nutrient status. The cell quota model estimates intracellular nitrogen $e_N$ (Eq. (6)) and phosphorus $e_P$ (Eq. (7)) fractions as function of three reference values of nutrient/carbon quota — internal nutrient/carbon ratio, minimum nutrient/carbon ratio and critical nutrient/carbon ratio or Redfield ratio (Bach, 1993; Baretta-Bekker et al. 1997)

$$f(N) = \min(e_N, e_P) \quad (5)$$

where

$$e_N = p\left[0, \frac{(X_N - X_N^{min})}{(X_N^R - X_N^{min})}, 1\right] \quad (6)$$

$$e_P = p\left[0, \frac{(X_P - X_P^{min})}{(X_P^R - X_P^{min})}, 1\right] \quad (7)$$

and $p(a, x, b) = \min[b, \max(a, x)]$; $X_N$, intracellular N/C ratio; $X_N^{min}$, N/C content of the structural parts of the cell; $X_N^R$, critical N/C ratio (Redfield ratio); $X_P$, intracellular P/C ratio; $X_P^{min}$, P/C content of the structural parts of the cell; $X_P^R$, intracellular P/C ratio.

Table 1
Comparison of several salt marsh systems around the world

| System | Tidal range | Salt marsh area (ha) | Vegetation | | References |
|---|---|---|---|---|---|
| | | | Lower marsh | Upper marsh | |
| Tagus estuary, Portugal | Mesotidal | 2000 | *Spartina maritima*, *Scirpus maritimus* | *Halimione portulacoides*, *Arthrocnemum fruticosum* | Crespo, 1993 |
| San Francisco Bay, US | Microtidal | 14760 | *Spartina* sp. | *Salicornia* sp., *Frankenia* sp., *Grindelia* sp., *Distichilis* sp. | Oceanus™, SFEP, 1992; Wright and Philips, 1988 |
| Severn estuary, UK | Macrotidal | 770[a] | *Spartina* sp. | *Puccinellia* sp. | Randerson, 1985 |
| North Inlet estuary, US | Microtidal | 3200 | *Spartina alterniflora* (tall forms) | *Spartina alterniflora* (short forms) | Dame and Kenny, 1986 |
| Oosterschelde, Netherlands | Mesotidal | 1725 | *Spartina* sp. | *Spartina* sp., *Puccinellia* sp., *Halimione* sp., *Elymus* sp. | Dejong et al., 1994 |
| Swartkops estuary, South Africa | Microtidal | 363 | *Spartina maritima*[a] | – | Pierce, 1983 |

[a] Lower salt marsh only.

Table 2
Parameter values used in the biomass production model

| Name | Units | Meaning | Values | References |
|---|---|---|---|---|
| $P_{max}$ | gC g dw $m^{-2}$ $h^{-1}$ | $C_3$ maximum production | 0.0023 | Dejong et al., 1982 |
| | | $C_4$ maximum production | 0.0036 | Catarino et al., 1985 |
| | | Allometric maximum production for weight class (1) | 0.016 | [a] |
| | | (2) | 0.011 | |
| | | (3) | 0.0054 | |
| | | (4) in lower marsh vegetation | 0.0036 | |
| $P_{max\ wt}$ | gC g dw $m^{-2}$ $h^{-1}$ | Allometric maximum production for weight class (1), (2), (3) and (4) in upper marsh vegetation | 0.0023 | Dejong et al., 1982 |
| $I_k$ | W $m^{-2}$ | $C_3$ light half-saturation constant | 150 | Dejong et al., 1982 |
| | | $C_4$ light half-saturation constant | 300 | Dejong et al., 1982; Morris, 1982 |
| $\theta_1$ | $h^{-1}$ | Temperature coefficient for growth | 1.08 | Bach, 1993 |
| $\theta_2$ | $h^{-1}$ | Temperature coefficient for growth | 1.07 | Bach, 1993 |
| $T_{opt}$ | °C | Temperature optimum | 25 | [a] |
| $X_n$ | – | Internal N/C | 0.063 | [a] |
| $X_n^{min}$ | – | Minimum N/C | 0.04 | Bach, 1993 |
| $X_n^R$ | – | Critical N/C | 0.06 | Bach, 1993 |
| $X_p$ | – | Internal P/C | 0.0062 | [a] |
| $X_p^{mina}$ | – | Minimum P/C | 0.004 | Bach, 1993 |
| $X_p^{Ra}$ | – | Critical P/C | 0.006 | Bach, 1993 |
| $q^{ex}$ | – | Exudation under nutrient stress | 0.2 | Bach, 1993 |
| $r^{bas}$ | $h^{-1}$ | Basal respiration ($C_3$) | $3.5\times10^{-5}$ | [a] |
| | | Basal respiration ($C_4$) | $2.3\times10^{-5}$ | [a] |
| $Q_{10}$ | – | $Q_{10}$ value | 2 | Baretta-Bekker et al., 1997 |
| $q^{res}$ | – | Respired fraction of production | 0.1 | Baretta-Bekker et al., 1997 |
| $W_1$ | $h^{-1}$ | Coefficient for $H$ (Eq. (11)) | 30 | Bach, 1993 |
| $W_2$ | $m^{-1}$ | Coefficient for $H$ (Eq. (11)) | 1.5 | Bach, 1993 |
| $L_{max}$ | GC gdw $h^{-1}$ | Maximum $L_m$ rate ($C_3$) | $2.3\times10^{-4}$ | [a] |
| $L_{max}$ | GC gdw $h^{-1}$ | Maximum $L_m$ rate ($C_4$) | $1.2\times10^{-4}$ | [a] |

[a] Values estimated at calibration.

Exudation, respiration and leaf mortality are sink terms in individual gross production (Eq. (1)). When the water rises salt marsh plants lose a few percent of the photosynthetic products, as dissolved organic carbon (DOC), to the water (Pomeroy et al., 1977). The excreted fraction ($E$) of gross production, exudation, is modelled as the sum of an activity excretion $P_g \cdot q^{ex}$ and the nutrient-stressed excretion (Eq. (6)), which is proportional to $1-f(N)$ (Baretta-Bekker et al., 1997)

$$E = P_g \cdot [q^{ex} + (1 - q^{ex}) \cdot (1 - f(N))] \quad (8)$$

where $q^{ex}$, fraction of gross production, which is excreted under nutrient-stressed conditions.

Without nutrient limitation $f(N) = 1$, exudation is a fraction of gross production. With total nutrient limitation $f(N) = 0$, exudation becomes equal to gross production, which means that all the photosynthetic products are being converted to DOC and no biomass growth occurs.

Respiratory losses described by Eq. (9) consist of a basal temperature-dependent respiration $r^{bas} \cdot [Q_{10}^{T/(T_{opt}-1)}]$ and activity respiration $q^{res} \cdot (P - E)$, which act only on assimilated biomass $P_g - E$ (Baretta-Bekker et al., 1997)

$$R = r^{\mathrm{bas}} \cdot Q_{10}^{T/(T_{\mathrm{opt}}-1)} + q^{\mathrm{res}} \cdot (P_{\mathrm{g}} - E) \quad (9)$$

where $r^{\mathrm{bas}}$, basal respiration; $Q_{10}$, $Q_{10}$ value; $q^{\mathrm{res}}$, respired fraction of production.

Leaf mortality is also a temperature-dependent function (Eq. (10)). The action of the tides and wave motion on leaf breakage is simulated through Eq. (11), where loss of above ground biomass $H$ increases with decreasing water height, expressing the greater effect of wave impact in shallow waters.

$$L_{\mathrm{m}} = L_{\max}(\theta_2^{T-T_{\mathrm{opt}}}) \cdot H \quad (10)$$

where $L_{\max}$, maximum leaf mortality rate; $\theta_2$, temperature coefficient for leaf mortality;

$$H = 1 + W_1 \cdot \mathrm{e}^{-W_2 \cdot h} \quad (11)$$

where $H$, loss of above ground biomass due to wave motion; $W_1$ and $W_2$, constants estimated at calibration (Bach, 1993); $h$, tidal height.

### 2.2.2. Demographic model

Population dynamics was simulated through a class transition model (Press et al., 1995; Ferreira et al., 1998). This sub-model simulates the transition of the individuals between weight classes in order to describe plant population density per unit area. Class transition is expressed by Eq. (12).

$$\frac{\partial n(s,t)}{\partial t} = -\frac{\partial [n(s,t)g(s,t)]}{\partial s} - \mu[(s)n(s,t)] \quad (12)$$

where $t$, time; $s$, weight class; $n$, number of individuals; $g$, scope for growth (growth rate); $\mu$, mortality rate.

The number of plants in each weight class depends on the individual scope for growth and on an allometric natural mortality rate. Additionally, erosion losses in the number of individuals are higher for lower weight classes (Table 3), i.e. physical resistance is also simulated allometrically. Recruitment to class 1 is explicitly modelled as a source of new recruits to the population. This is due to the reproduction in weight class 4, and decreases individual scope for growth in this weight class during the reproductive period.

### 2.2.3. Model calibration and validation

The model was implemented using the Powersim™ software, and was calibrated independently for $C_3$ and $C_4$ plants. Carbon is used as the central model unit, and simulations were run with a time step of 1 h, over a period of 110 years. The parameters used in the biogeochemical and demographic models are presented in Table 2 and Table 3, respectively.

The comparison between the model results obtained for total biomass, production and density, and the field data for these variables were used to validate the model. Model results for the $C_4$ photosynthesis pathway were compared with field data obtained for *Spartina maritima* (lower marsh) while $C_3$ model results were compared

Table 3
Parameter values used in the demographic model

| Name | Units | Meaning | Lower marsh | Upper marsh |
|---|---|---|---|---|
| $S_1$ | g dw | Mean dry weight class 1 | 1.0 | 1.0 |
| $S_2$ | | Mean dry weight class 2 | 1.5 | 1.5 |
| $S_3$ | | Mean dry weight class 3 | 2.0 | 2.0 |
| $S_4$ | | Mean dry weight class 4 | 2.5 | 2.5 |
| $Wt_1$ | Ind $m^{-2}$ | Weight class 1 | 600 | 1600 |
| $Wt_2$ | | Weight class 2 | 188 | 700 |
| $Wt_3$ | | Weight class 3 | 50 | 200 |
| $Wt_4$ | | Weight class 4 | 100 | 100 |
| $\mu_1$ | $h^{-1}$ | Mortality rate in weight class 1 | $0.3/1+e^{(4-0.015*n_1)_a}$ | $0.25/1+e^{(6-0.004*n_1)_a}$ |
| $\mu_2$ | | Mortality rate in weight class 2 | $0.05/1+e^{(5-0.04*n_2)_a}$ | $0.016/1+e^{(7.5-0.012*n_2)_a}$ |
| $\mu_3$ | | Mortality rate in weight class 3 | $0.01/1+e^{(6.5-0.08*n_3)_a}$ | $0.0076/1+e^{(6.2-0.027*n_3)_a}$ |
| $\mu_4$ | | Mortality rate in weight class 4 | $0.012/1+e^{(8-0.07*n_4)_a}$ | $0.00005/1+e^{(11-0.08*n_4)_a}$ |

[a] $n_i$, number of individuals in weight class $i$ ($i = 1$, 2, 3 or 4, respectively).

with field data averaged from *Arthrocnemum fruticosum* and *Halimione portulacoides* (upper marsh).

### 2.3. Geographical information analysis

#### 2.3.1. Bathymetry data

The bathymetry data available for the Tagus estuary consists of a grid with 300 m resolution, generated by the Hydrographical Institute of the Portuguese Navy from in situ depth measurements. This table was used in 1992 to create the navigation charts for the Tagus estuary, which means the data was gathered around 1990. The grid is projected in the Portuguese Gauss-Military system.

#### 2.3.2. Salt marsh data

The determination of salt marsh areas was achieved through remote sensing. The data came from a Landsat image of the Tagus estuary with a resolution of 30 m per pixel, taken in 1991 at low spring tide; this means it contains all the estuarine intertidal area. The image was rectified in order to fit into Portuguese military co-ordinates; ground control points were collected from the bathymetry map in order to achieve the best matching with the existing data. All image treatment was executed with ER Mapper™.

Salt marsh area was defined using a Normalised Differential Vegetation Index (NDVI). According to several authors (for example, Goward et al., 1985; Zhang et al., 1997), vegetation can be highlighted from multi-spectral images using vegetation indices. These indices are generated by the combination of remote sensing bands (usually in the red and near infrared spectrums) to highlight information on vegetation location and abundance. NDVI is based on the high absorption of energy by vegetation pigments in the red and low absorption in the near-infrared spectral range and can be calculated as

$$\mathrm{NDVI} = \frac{\mathrm{Near\_Infrared} - \mathrm{Red}}{\mathrm{Near\_Infrared} + \mathrm{Red}}$$

(Modified from Goward et al., 1985). (13)

NDVI and similar indexes have been used extensively for salt marsh zonation and classification (Zhang et al., 1997).

From the NDVI results, enhanced to display only the study area, salt marshes were defined with a GIS. There is a clear difference between salt marsh and surrounding area in terms of vegetation density (Eleuterius and Eleuterius, 1979), which allows a clear differentiation between both. The area was then quantified using tools from the GIS software.

#### 2.3.3. Sea-level rise scenarios

According to Allen (Allen 1990a,b, 1995, 1997) the relative elevation to tidal datum of the surface of a salt marsh at a place ($\eta$) changes annually with 'natural' sea-level rise due to mineral and organic accretion, which includes natural subsidence, soil compaction and depletion of groundwater levels, and sea-level rise due to climate change

$$\frac{\partial \eta}{\partial t} = \partial S_{\mathrm{min}} + \partial S_{\mathrm{org}} - \partial M - \partial P \qquad (14)$$

where $t$, time; $S_{\mathrm{min}}$, the thickness of added minerogenic sediment; $S_{\mathrm{org}}$, the thickness of added organogenic sediment; $M$, the change in relative sea-level (positive upward); $P$, change in the position of the marsh surface due to longe-range compaction.

To simulate the gradual water elevation deficit in the study area during the simulation period, a simple model was developed taking into account the process referred above. The model was coupled with the production module in order to reflect the effects of water elevation on lower and upper salt marsh vegetation.

Due to the lack of data on mineral and organic accretion in the study area, a constant annual sedimentation rate was used. The sedimentation rate for the Tagus estuary was estimated as 0.77 cm per year for the study area (Castanheiro and Relvas, 1985). Natural sea-level rise has been estimated as 0.18 cm per year (Titus and Narayanan, 1995). The water rise scenarios proposed by IPCC (1995) were chosen for this study. IPCC estimates a sea-level rise due to climate change, from 1990 to 2100, to be about 50 cm, or

Table 4
Comparison between model results and field data for lower and upper marsh density, biomass and production[a]

| Zonation | Observed values | | Model results | |
|---|---|---|---|---|
| | Lower marsh | Upper marsh | Lower marsh | Upper marsh |
| Density (stems $m^{-2}$) | – (500–2500) | – | 480 (260–860) | 2500 (1645–3457) |
| Biomass (g $m^{-2}$) | 924 (417–1417) | 3337 (2271–4522) | 850 (544–1342) | 3240 (2198–4298) |
| Production (g $m^{-2}$ per year) | 670 | 1900[b] | 600 | 1800 |

[a] Field observed data were taken from Catarino (1981) and Catarino and Caçador (1981). Values between brackets correspond to the range of observed and predicted data.
[b] Mean value obtained for *Arthrocnemum fruticosum* and *Halimione portulacoides*.

0.45 cm per year. The 'high sea-level rise' scenario presented corresponds to a 95 cm rise, or 0.86 cm per year (IPCC, 1995, 1999). Both scenarios were studied due to the high uncertainty surrounding this issue. A linear increase in this variable was considered during the simulation period.

## 3. Results and discussion

### 3.1. Model results per unit of area

The results of the main model state variables in the standard simulation are presented in Table 4. The comparison between model results and field data shows that simulated density, biomass and production fall within the range observed by Catarino (1981) and Catarino and Caçador (1981), although the model slightly overestimates measured data of biomass and production for lower marsh vegetation.

Observed and simulated biomass per unit area over 1 year is represented in Fig. 2. The correlation between these two variables is positive and significant ($P < 0.01$).

### 3.2. Model upscaling

#### 3.2.1. Spatial analysis of salt marshes

Fig. 3 shows the NDVI derived from the Landsat image. The NDVI has been classified into 256 classes corresponding to vegetation density, with higher classes (darker colours) representing higher density. As can be seen in the figure, the difference in vegetation density between salt marsh and non-salt marsh areas is clear enough to allow an easy delimitation of the area. This is especially true for the differentiation between salt marshes and tidal flats. Therefore, zonation of salt marshes was achieved by means of photo-interpretation. The total salt marsh area was calculated to be 1876 ha.

A comparison was made with the earlier salt marsh zonation by Crespo (1993) in order to confirm the results obtained using the NDVI. Crespo conducted a supervised classification of a SPOT satellite image from 1986, determining total marsh area as being 1998 ha. Crespo also compared classification results with existing salt marsh cartography from 1980, which determined total marsh area as being 1938 ha. These two methods also showed very similar results in locating salt marsh areas.

This study obtained very similar results to both the SPOT data and the cartography. Not only are the salt marsh areas very similar in size, they are also located in the same regions. The small difference in area size is probably due to the fact that Crespo's analysis includes a small salt marsh area to the south of the estuary not included in the present study. Therefore, confirmation of NDVI methodology for the Tagus estuary is accepted in both salt marsh location and area determination.

#### 3.2.2. Relation between salt marsh zonation and tidal level

Knowledge of the relation between tidal levels and salt marsh zonation is useful to determine the impact of sea-level rise on salt marshes with different elevations above tidal datum. In salt

marshes with large tidal amplitudes, the lower height of the salt marsh is expected to be slightly above the mean low tide (Eleuterius and Eleuterius, 1979). A probable reason is that, in these estuaries, plants near the mean low tide line are more often below water than in estuaries with low tidal amplitude. The Tagus estuary has an average tidal amplitude of about 2.5 m (determined with the Oceanus™ software), which means it can be classified in this range. The mean low tide for the estuary is 0.95 m, so salt marshes may be expected to occur above this level.

Fig. 4 shows the distribution of salt marsh areas by height classes, above the mean low tide; average salt marsh height is 1.64 m above tidal datum. An analysis of the image shows two groups of salt marsh, one between 0.9 and 1.5 m; and one above 1.5 m. Only 65% of the salt marshes are represented in this chart, however, due to problems in correlating the high-resolution satellite image with the more coarse bathymetry data. Of the remaining 35%, it is only possible to determine if they are below or above the 1.5 m line (6% are located below 1.5 m while 29% are located above this level).

In order to explain this separation in height classes, it must be considered that this could represent domination either by lower marsh plant species or upper marsh plant species, since the former prefer areas with frequent exposure periods, while the latter usually occupy areas with frequent submersion periods (Eleuterius and Eleuterius, 1979).

A comparison with existing cartography in Crespo (1993) was impossible due to the fact that there is no clear differentiation between lower marsh and upper marsh plants. However, Catarino (1981) determined lower marsh and upper marsh plant areas to be, respectively, 72 and 28% of the total

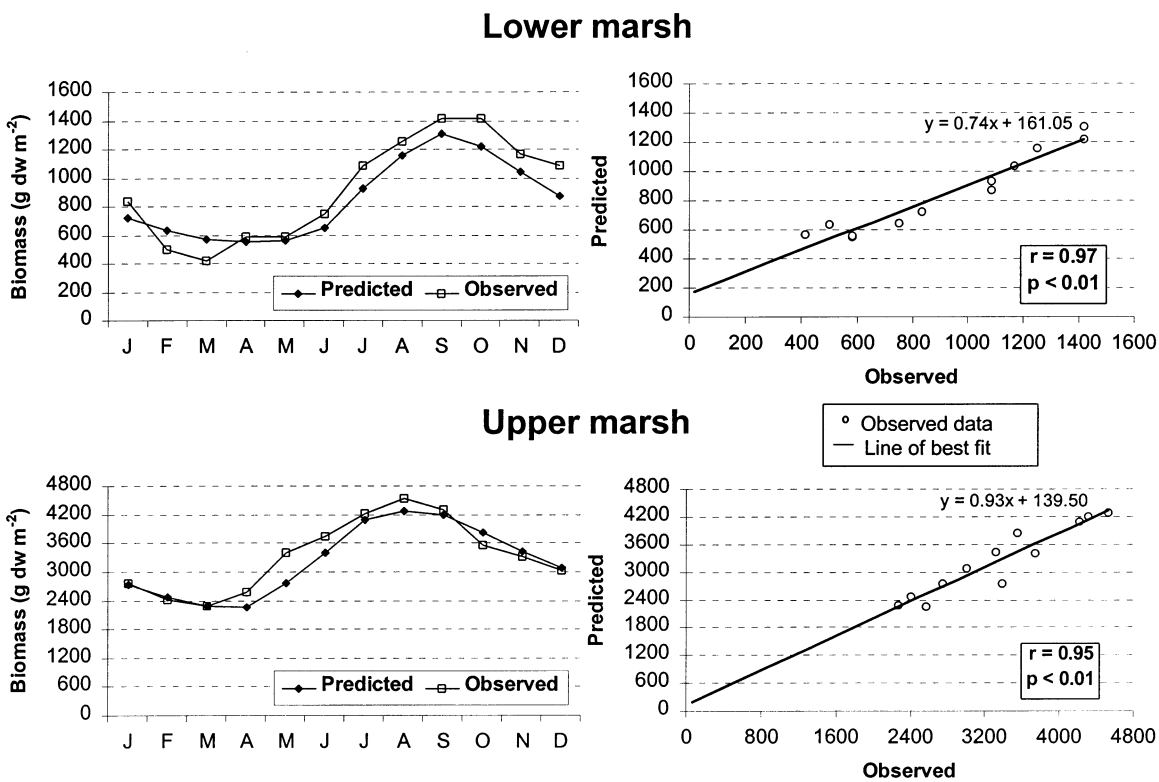


Fig. 3. NDVI derived from satellite image (darker colours represent higher vegetation density). Study site location is also shown.

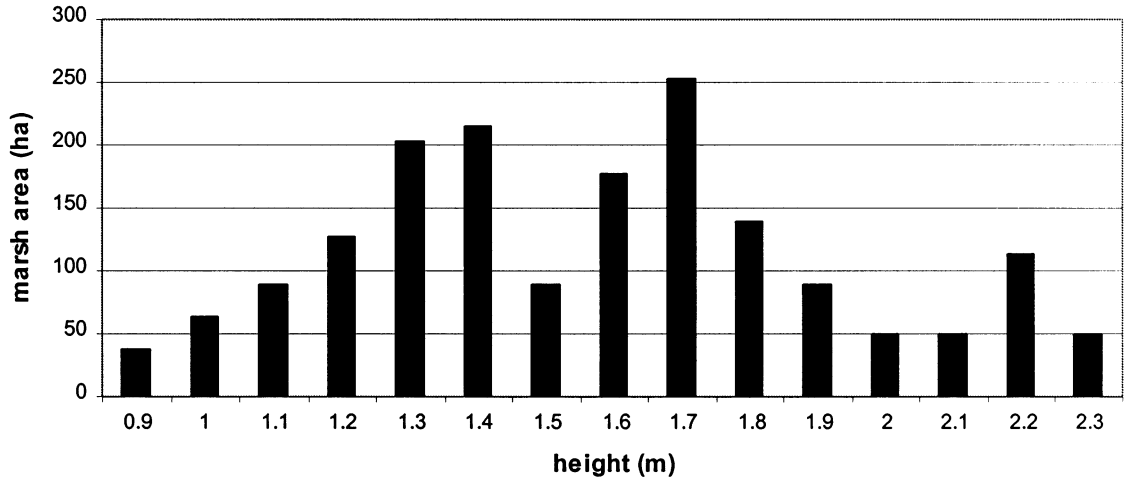


Fig. 4. Distribution of salt marsh areas according to height.

salt marsh area in the Tagus estuary. The similarity between the lower marsh and upper marsh areas determined by Catarino (1981) (525 and 1351 ha, respectively) and the ones determined to be below or above 1.5 m (675 and 1201 ha, respectively), leads to the conclusion that there is a relationship between these two factors. Therefore, this study considers that salt marsh areas located below 1.5 m are dominated by lower marsh vegetation, while upper marsh plants dominate areas located above this level (Table 5). This conclusion is supported by the work of Eleuterius and Eleuterius (1979) in determining the influence of tidal height in upper and lower salt marsh zonation.

### 3.2.3. Modelling of total salt marsh production

Modelling of the sea-level rise effects was made using only the high estimate scenario of sea-level rise (95 cm) discussed above, since the modelled sediment deposition for the best estimate scenario was above the projected sea-level rise (50 cm) in 2100.

Lower and upper marsh areas were simulated using the $C_4$ and $C_3$ models, respectively, due to the fact that one $C_4$ species dominates the lower marsh, while two $C_3$ species dominate the upper marsh. Total plant production of the system, calculated by upscaling the ecological model using the GIS areas, can be used to discuss the role played by salt marsh plants on nutrient removal from the system. The population equivalent values used for nutrients were 4380 g N and 1022 g P per inhabitant per year. Thus, the salt marsh production is responsible for the annual removal of about 1200 tonnes of nitrogen and 170 tonnes of phosphorus, which corresponds to roughly 270 000 inhabitants and 170 000 inhabitants, respectively.

Fig. 5 shows the model results obtained for vegetation density of both lower and upper salt marshes (from 1990 to 2100) in both sea-level rise scenarios considered, 0 and 95 cm in 2100. The number of individuals in both marsh zones decreases over the simulated years and tends towards zero, especially for plants of the lower marsh.

The values of total salt marsh production and biomass calculated by the model for both scenarios are presented in Fig. 6. In 2100, the model predicts losses in biomass and production of

Table 5
Scenario characteristics

| | Lower marsh | Upper marsh |
|---|---|---|
| Total area (ha) | 1201 | 675 |
| Average height in 1990 (m) | 1.85 | 1.28 |
| Average height in 2100 (m) | 1.55 | 0.98 |

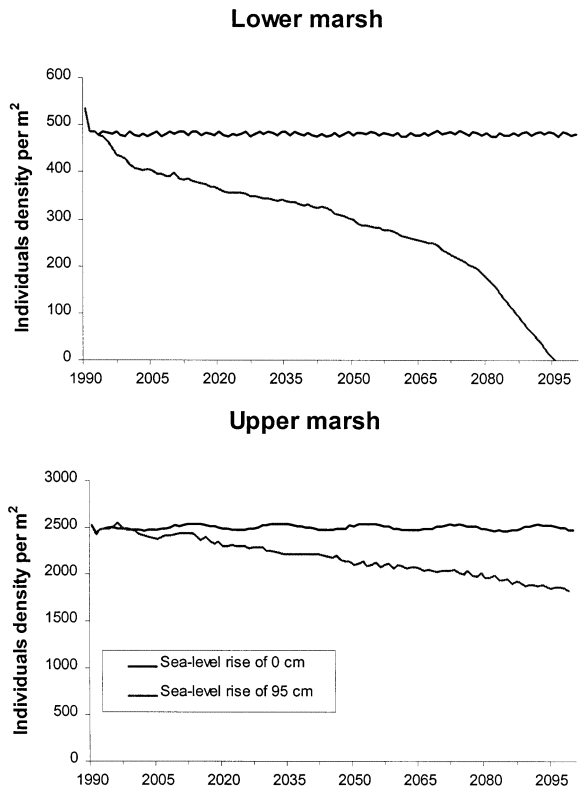


Fig. 5. Model results for annual density variation in lower and upper marsh vegetation for both simulated scenarios of sea-level rise. It is important to note that the results obtained for the 2100 scenarios correspond to the direct application of sea level rise values considering that no new colonisation would take place.

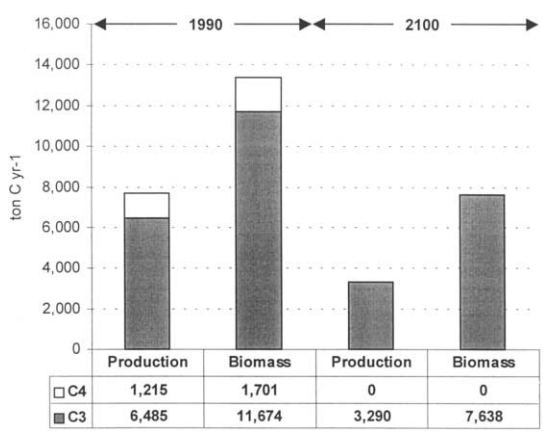


Fig. 6. Model results of total biomass and production in lower and upper marsh for both scenarios proposed.

about 100% of the actual plant marsh production in the lower marsh, which means that by 2100 the present day lower salt marsh may potentially disappear. In the same scenario at the end of the last simulated year, the upper marsh biomass will decrease by 35% while production losses will reach 50%. This result can be due to plant marsh zonation since pioneer species of the lower marsh are the first vertical colonisers and the first to be inundated. It must also be remembered that the model does not consider any colonisation made by lower marsh vegetation in areas earlier dominated by upper marsh plants.

### *3.3. Salt marsh loss — spatial risk assessment*

In order to determine the susceptibility to submersion of different salt marsh areas in the estuary, a risk assessment was carried out. This assessment was based on the two sea-level rise scenarios discussed above. IPCCs best estimate, which indicates no loss of salt marsh area, was considered the most likely scenario; and IPCCs high estimate, which indicates the complete loss of salt marsh area, was considered the least likely. It was assumed that the lowest regions of marsh would be the first to disappear, and that no new colonisation would take place, since the amount of newly created wetlands will be much smaller than the area of wetlands that are lost (EPA, 1999). Fig. 7 presents the results of this analysis, carried out for the following four risk classes:

- Very High Risk: the lowest 25% of salt marsh area (0.9–1.4 m);
- High Risk: 25–50% of salt marsh area (1.4–1.7 m);
- Moderate Risk: 50–75% of salt marsh area (1.7–1.9 m);
- Low Risk: 75–100% of marsh area (1.9–2.3 m).

The eastern salt marsh area is the most resistant, due to its higher elevation, and most of the area has a moderate to low risk of destruction. Conversely, the lower salt marsh areas in the north and west of the estuary present high to very high risk.

## 4. Conclusions

The methodology developed in this study integrates biogeochemical and demographic modelling, remote sensing and geographical information analysis. Feedback components between the small-scale simulation and marsh-scale processes were also introduced.

The key information was determined to be the bathymetry, plant zonation (in this case differentiated by vegetation type and height class), and data on vegetation density and productivity. The use of a combined biogeochemical and demographic model to represent the small-scale biomass dynamics provides a way to include meaningful abiotic forcing in the production model, whilst retaining the frequently important differentiation between cohorts, e.g. insofar as reproduction and recruitment is concerned. Improvements, which must be considered, include a better description of nutrient availability and the simulation of the salt marsh below-ground biomass.

The coupled model developed in this work provides a robust methodology for analysis of the effects of global change on benthic primary production of coastal areas, not only for halophytic vegetation, but (with some modifications in the description of productive processes) also for macrophyte algae, seagrasses and mangroves.

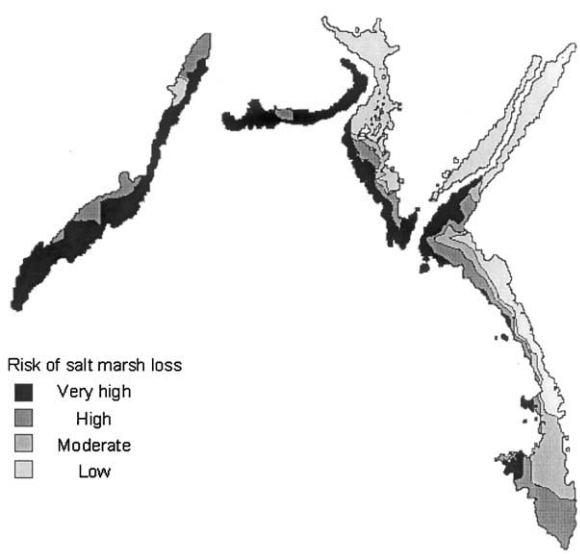


Fig. 7. Results of the risk assessment for the losses in salt marsh areas of the Tagus estuary.

## Acknowledgements

This work was funded by the European Commission Environment Programme, contract N° ENV4-CT97-0436 (EUROSAM) and FESTA project. T. Simas acknowledges MSc. and Ph.D. research grants from FCT-MCT in Portugal. The authors wish to thank B. Bodo for his work with the satellite image, J.L. Silva for his insights on remote sensing, and R. Neves for supplying the bathymetry. Helpful comments by two anonymous reviewers are also acknowledged.

## References

Allen, J.R.L., 1990a. The formation of coastal peat marshes under an upward tendency of relative sea-level. J. Geol. Soc. 147, 743–745.

Allen, J.R.L., 1990b. Salt-marsh growth and stratification: a numerical model with special reference to the Severn Estuary, southwest Britain. Mar. Geol. 95, 77–96.

Allen, J.R.L., 1994. A continuity-based sedimentological model for temperate-zone tidal salt marshes. J. Geol. Soc. 151, 41–49.

Allen, J.R.L., 1995. Salt-marsh growth and fluctuating sea-level: implications of a simulation model for Flandrian coastal stratigraphy and peat-based sea-level curves. Sed. Geol. 100, 21–45.

Allen, J.R.L., 1997. Simulation models of salt-marsh morphodynamics: some implications for high-intertidal sediment couplets related to sea-level change. Sed. Geol. 113, 211–223.

Bach, H.K., 1993. A dynamic model describing the seasonal variations in growth and the distribution of ellgrass (*Zostera marina* L.). I. Model theory. Ecol. Model. 65, 31–50.

Baretta-Bekker, J.G., Baretta, J.W., Ebenhoh, W., 1997. Microbial dynamics in the marine ecosystem model ERSEM II with decoupled carbon assimilation and nutrient uptake. J Sea Res. 38, 195–211.

Berner, E.K., Berner, R.A., 1996. Global Environment: Water, Air and Geochemical Cycles. Prentice-Hall, USA.

Boumans, R.M.J., Day, J.W. Jr, 1993. High precision measurements of sediment elevation in shallow coastal areas using a sedimentation-erosion table. Estuaries 16 (2), 375–380.

Brock, T.D., 1981. Calculating solar radiation for ecological studies. Ecol. Model. 14, 1–19.

Caçador, M.I.V., 1994. Acumulação e retenção de metais pesados nos sapais do estuário do Tejo. Dissertação de doutoramento. Faculdade de Ciências — Universidade de Lisboa, Portugal, pp. 142.

Cahoon, D.R., Lynch, J.C., Powell, A.N., 1995. Marsh vertical accretion in a southern Califronia estuary, USA. Est. Coast. Shelf Sci. 43, 19–32.

Castanheiro, J., Relvas, P., 1985. Evolução dos fundos do estuário do Tejo. Estudo ambiental do estuário do Tejo UNDP/POR/77/016. Direcção Geral da Qualidade do Ambiente, Portugal.

Catarino, F., 1981. Papel das zonas húmidas do tipo sapal na descontaminação das águas. Ciência 1, 2 IV série.

Catarino, F.M., Caçador, M.I., 1981. Produção de biomassa e estratégia do desenvolvimento em Spartina maritima e outros elementos da vegetação dos sapais do estuário do Tejo. Bol. Soc. Sér. 2 (54), 387–403.

Catarino, F., Tenhumen, J.D., Brotas, V., Lange, O.L., 1985. Application of $CO_2$-porometer methods to assessment of components of photosynthetic production in estuarine ecosystems. Mar. Biol. 89, 37–43.

Crespo, R., 1993. Cartografia do habitat potencial de passeriformes no Estuário do Tejo por processamento digital de imagem. Relatório de estágio de Licenciatura. Faculdade de Ciências — Universidade de Lisboa, Portugal, pp. 124.

Day, J.W. Jr, Rybczyk, J., Scarton, F., Rismondo, A., Are, D., Cecconi, G., 1999. Soil accretionary dynamics, sea-level rise and the survival of wetlands in Venice lagoon: a field modelling approach. Est. Coast. Shelf Sci. 49, 607–628.

Dame, R.F., Kenny, P.D., 1986. Variability of *Spartina alterniflora* primary production in the euhaline North Inlet estuary. Mar. Ecol. Prog. Ser. 32, 71–80.

Dejong, T.M., Drake, B.G., Pearcy, R.W., 1982. Gas exchange responses of Chesapeake Bay tidal marsh species under field and laboratory conditions. Oecologia 52, 5–11.

Dejong, D.J., Dejong, Z., Mulder, J.P.M., 1994. Changes in Area, Geomorphology and Sediment Nature of Salt Marshes in the Oosterschelde Estuary (SW Netherlands) due to Tidal Changes. In: Hydrobiologia, 282/283, Kluwer Academic Publishers, Belgium, pp. 303–316.

Eleuterius, L.N., Eleuterius, C.K., 1979. Tide levels and salt marsh zonation. Bull. Mar. Sci. 29 (3), 394–400.

EPA (US Environment Protection Agency), 1999. http://www.epa.gov/globalwarming/impacts/coastal/index.html.

Ferreira, J.G., Duarte, P., Ball, B., 1998. Trophic capacity of Calingford Lough for oyster culture — analysis by ecological modelling. Aquat. Ecol. 31, 361–378.

Gates, D.M., 1993. Climate Change and its Biological Consequences. Sinauer Associates, Inc, USA.

Goward, S.N., Tucker, C.J., Dye, D.G., 1985. North American vegetation patterns observed with the NOAA-7 advanced very high resolution radiometer. Vegetatio 64, 3–14.

Hackney, C.T., Cleary, W.J., 1987. Saltmarsh loss in Southeastern North Carolina Lagoons: importance of sea-level rise and inlet dredging. J. Coast. Res. 3 (1), 93–97.

Houghton, J., 1999. Global Warming: The Complete Briefing, Second edition. Cambridge University Press, UK, p. 251.

Intergovernmental Panel on Climate Change (IPCC), 1990. Climate change. In: Houghton, J.T., Jenkins G.J., Ephraumus J.J. (Eds.), The IPCC Assessment. Cambridge University Press, UK. http://www.ipcc.ch/pub/reports.htm.

Intergovernmental Panel on Climate Change (IPCC), 1995. Climate Change 1995, The IPCC Second Assessment Synthesis of Scientific-Technical Information Relevant to Interpreting Article 2 of the UN Framework Convention on Climate Change. IPCC, Switzerland. http://www.ipcc.ch/pub/reports.htm.

Intergovernmental Panel on Climate Change (IPCC), 1999. Aviation and the global atmosphere. A special report of working groups I and III of the Intergovernmental Panel on Climate Change. Summary for policymakers. IPCC, Switzerland. http://www.ipcc.ch/pub/reports.htm.

Morris, J.T., 1982. A model of growth responses by *Spartina alterniflora* to nitrogen limitation. J. Ecol. 70, 25–42.

Nyman, J.A., DeLaune, R.D., Roberts, H.H., Patrick, W.H. Jr, 1993. Relationship between vegetation and soil formation in a rapidly submerging coastal salt marsh. Mar. Ecol. Prog. Ser. 96, 269–279.

Nyman, J.A., Carloss, M., DeLaune, R.D., Patrick, W.H. Jr, 1994. Erosion rather than plant dieback as the mechanism of marsh loss in an estuarine marsh. Earth Surf. Proc. Landf. 19, 69–84.

Pierce, S.M., 1983. Estimation of the non-seasonal production of *Spartina maritima* (Curtis) Fernald in a South African estuary. Est. Coast. Shelf Sci. 16, 241–254.

Pomeroy, L.R., Bancroft, K., Breed, J., Christian, R.R., Frankenberg, D., Hall, J.R., Maurer, L.G., Wiebe, W.J., Wiegert, R.G., Wetzel, R.L., 1977. Flux of organic matter through a salt marsh. Estuarine processes. In: Circulation, Sediments and Transfer of Material in the Estuary, vol. 2. Academic Press, USA, pp. 270–279.

Press, W.H., Teukolsky, S.A., Vetterling, W.T., Flannery, B.P., 1995. Numerical recipes in C — The art of Scientific Computing. Cambridge University Press, UK.

Randerson, P.F., 1985. A model of carbon flow in the Spartina Anglica Marshes of the Severn Estuary UK. In: Estuarine Variability. Academic Press, New York, pp. 427–446.

Reed, D.J., 1990. The impact of sea-level rise on coastal salt marshes. Prog. Phys. Geog. 14 (4), 465–481.

Reed, D.J., Foote, A.L., 1997. Effect of hydrologic management on marsh surface sediment deposition in coastal Louisiana. Estuaries 20 (2), 301–311.

San Francisco Estuary Project (SFEP) 1992. State of the Estuary Report. A Report on Conditions and Problems in the San Francisco Bay/Sacramento-San Joaquin Delta Estuary. SFEP, USA. http://www.abag.ca.gov/bayarea/sfep/sfep.html.

Stevenson, J.C., Ward, L.G., Kearney, M.S., 1986. Vertical accretion in marshes with varying rates of sea-level rise. In: Wolfe, D.A. (Ed.), Estuarine Variability. Academic press, Orlando, pp. 241–259.

Titus, J.G., Narayanan, V.K. 1995. The probability of Sea-level Rise. Environmental Protection Agency, USA. http://users.erols.com/jtitus/Holding/NRJ.html.

Titus, J.G., Park, R.A., Leatherman, S.P., Weggel, J.R., Greene, M.S., Mausel, P.W., Brown, S., Gaunt, C., Trehan, M., Yohe, G., 1991. Greenhouse effect and sea-level rise: the cost of holding back the sea. Coast. Manage. 19, 171–210.

Van Dijkeman, K.S., Bossinade, J.H., Bouwema, P., Glopper, R.J., 1990. Salt marshes in the Netherlands Wadden Sea: rising high-tide levels and accrettion enhancement. In: Expected Effects of Climatic Change on Marine Coastal Ecosystems. Kluwer Academic Publishers, The Netherlands, pp. 173–188.

Woolnough, S.J., Allen, S.R.J., Wood, W.L., 1995. An exploratory numerical model of sediment deposition over tidal salt marshes. Est. Coast. Shelf Sci. 41, 515–543.

Wright, D.A., Philips, D.J.H., 1988. Chesapeake and San Francisco Bays. A study in contrasts and parallels. Mar. Pol. Bull. 19 (9), 405–413.

Zhang, M., Ustin, S.L., Rejmankova, E., Sanderson, E.W., 1997. Monitoring Pacific Coast saltmarshes using remote sensing. Ecol. Appl. 7 (3), 1039–1053.